

Measurement and Modeling of Short Copper Cables for Ultra-Wideband Communication

Thomas Magesacher,^a Jaume Rius i Riu,^{a,b} Miloš Jakovljević,^c Murilo Loiola,^d Per Ödling,^a and Per Ola Börjesson^a

^aDepartment of Information Technology, Lund University
P.O. Box 118, S-22100 Lund, Sweden

^bAccess Signal Processing Lab, Ericsson AB
P.O. Box 1505, S-12525 Stockholm, Sweden

^cETSI Telecomunicación, Universidad Politécnica de Madrid
Ciudad Universitaria s/n, 28040, Madrid, Spain

^dFEEC/DECOM, Universidade Estadual de Campinas
C.P. 6101, 13083-852 Campinas SP, Brazil

ABSTRACT

High-speed communication using the copper network, originally installed for telephony, is one of the dominant Internet access techniques. Several variants of a technology referred to as digital subscriber line (DSL) have been developed, standardized and installed during the last two decades. Essentially, DSL achieves high rates by exploiting wide bands of the copper cable channel. The shorter the cable, the wider the band that can be used efficiently for communication. Current DSL standards foresee the use of bands up to 30MHz. Cable properties have been studied by means of measurements, characterization and modeling up to frequencies of 30MHz.

Recent investigations have shown that it is feasible both from technical and from economical point of view to exploit very short cables (up to 200m) even further and use bands above 30MHz. A prerequisite for further evaluation and the design of such ultra-wideband copper (UWBC) systems is the extension of existing cable models to higher frequencies. This paper presents wideband measurement results of insertion loss and crosstalk coupling in a 10-pair cable of various length values for frequencies up to 200MHz. We compare the results with extrapolations of cable models that are established in the 30MHz-range.

Keywords: channel modeling, copper cable channel, crosstalk, DSL

1. INTRODUCTION

Digital subscriber line (DSL) is one of the most important Internet access technologies. The infrastructure of DSL is the copper network which has been installed and continuously extended during the last 120 years. The initial intention of the copper access plant was to enable speech transmission, often referred to as plain old telephone service (POTS). The key to achieve high data rates is exploiting wide bands of the copper cable channel. While voice transmission via POTS uses only the band from 300Hz to 3800Hz, various DSL technologies use bands in the frequency region from 25kHz to 30MHz.

The quality of the copper cable channel in terms of attenuation, unwanted noise and interference gradually decays as the frequency increases. Apart from increasing signal attenuation, typically quantified in terms of the so-called insertion loss,¹ also the electromagnetic coupling among pairs in a cable becomes significant. Remnants of the signals transmitted in neighboring pairs are detectable at each of the two ends of any pair in cable—an effect referred to as crosstalk. In case the crosstalk source is located at the same end of the cable as the “victim receiver”, this unwanted coupling and the resulting interference is referred to as near-end crosstalk (NEXT). In case the crosstalk source is located at the opposite end of the cable as the “victim receiver”, we speak about far-end crosstalk (FEXT).

Send correspondence to Thomas Magesacher (E-mail: thomas.magesacher@it.lth.se, Telephone: +46 46 222 7539)

Within the class of guided channels, the copper cable channel is by no means a favorable channel for high-rate data transmission (with rates of several tens of Mbit/s) in terms of transmission characteristics and immunity to interference. Its wide use is a consequence of the economic advantage of having the copper lines already installed almost everywhere.

The length of a copper pair from a central office, a cabinet, or from a distribution point to the remote terminal at the customer premises* determines the frequency range that can be used for communications in an economically sensible way. Although one could squeeze out a few bit/s of a 5km-loop by exploiting bandwidth beyond a few MHz, such an attempt would be of low economic value. These lengths are well covered by techniques like ADSL2plus. For short loops—around 1km—VDSL2 with its band plans that cover the frequency range up to 30MHz is sufficient. For very short loops (a few hundred meters), however, it is sensible both from technological and from economic point of view to go beyond the currently conjectured limit of 30MHz. While wireless LAN or Ethernet equipment might be the easier and preferred solution for the Intranet segment (e.g. a company's network covering one or a few floors of a skyscraper), there is still a potential for increasing the speed of Internet access over very short loops by using frequencies above 30MHz.

As a basis for the assessment and the development of such beyond-30MHz or ultra-wideband over copper techniques, it is necessary to reliably measure and characterize the response of the copper loops at those high frequencies. The present DSL technologies offer measurement techniques capable of characterizing DSL loops from one side (Single Ended Line Testing SELT²) or from both sides (Dual Ended Line Testing³⁻⁵). Both techniques can be used to estimate the particular characteristics of the DSL loops such as length, the presence and location of bridge taps, load coils, noise, the presence of short-circuits, etc. allowing providers to calculate approximately whether a loop will qualify for DSL services (cf.⁶ and references therein). These standardized techniques, however, at the present time cover the band from POTS frequencies up to 2.2MHz³⁻⁵. Thus, it is necessary to perform dedicated measurements in the high-frequency bands in order to generate reliable high frequency cables models for DSL loops.

The work presented in this paper provides experimental data from insertion loss and crosstalk coupling measurements in a 10-pair cable, for loops 50m and 200m long in a frequency band up to 200 MHz. The measurement results are compared with extrapolations of widely-used 30MHz-models. The paper is organized as follows. In Section 2, a review of 30MHz-models is presented. In Section 3, the conducted measurements and the measurement setup is explained. A comparison of ultra-wideband measurement results and extrapolated results derived from 30MHz-models is presented in Section 4. Section 5 concludes the work.

2. CABLE MODELS

2.1. Review of state-of-the-art models

A review of cable modeling basics in DSL can be found in⁷ and⁸. The earliest approach to modeling a pair of twisted wires is based on an equivalent two-port electrical circuit representing an infinitely small portion of a uniform line. The four parameters of this circuit (resistance R , inductance L , capacitance C , and conductance G) are referred to as primary parameters (or $RLCG$ parameters) of a loop. A lot of effort has been made to characterize these values for different loop diameters (cf. tables in¹). Closely connected to the $RLCG$ parameters are the characteristic impedance Z_0 and the propagation constant γ —both can be derived directly from the $RLCG$ parameters and vice versa. Z_0 and γ are also referred to as secondary parameters. Based on these secondary parameters is the two-port modeling approach—the so-called $ABCD$ model. The four 2×2 matrices A, B, C , and D describe the relation between input and output current/voltage of a two-port network representing a loop of a certain length. The elements of these four matrices can be derived directly from the secondary parameters. The $ABCD$ -model is particularly convenient for modeling of concatenated loop sections. Although frequently used, the $ABCD$ -model is only one out of many possibilities to model a single loop. All the theory mentioned above can be extended to multi-conductor systems modeling whole cables⁹—an approach that becomes more and more interesting as a basis for coordinated transmission and spectrum management techniques in order to exploit the copper cable as a whole.

The above modeling techniques are all based on the primary parameters and indeed represent one of the mainstream approaches: trying to characterize the primary parameters as accurately as possible. From there everything is possible—the model can predict different lengths and different terminations. Approaches to primary-parameter modeling include tabular collection of parameters based on huge databases of measurements as well as generic models for R, L, C , and G (all dependent on frequency).

*Such an end-to-end copper connection is often referred to as loop.

Virtually every major operator has created its own generic reference model in order to predict the insertion loss of the loops in the corresponding access network. These modeling approaches can be classified into two groups. The first group consists of models focusing on primary parameters (*RLCG*). Prominent examples for such models are the BT-model¹⁰ or the KPN-model¹¹. The second group focuses on the secondary parameters (Z_0, γ) and includes the DT-model¹² and the Swisscom-model¹³.

In general, all these reference models may exhibit physically impossible behaviors when viewed in the time domain. Examples of such effects are information traveling faster than light or non-causality (responses arrive before the excitation)¹⁴. As a result, these models are not a good reference for time domain representation of twisted pair loops. The model that first appeared to respect the causality is the MAR model¹⁵. Another recent model obeying causality is the VUB-model^{16,17}. Note that all the models mentioned above are unable to span a whole frequency range from DC to 30MHz without producing noticeable differences between the modeled and the measured results⁸. The European and the American standardization bodies, ETSI and ANSI, respectively, have defined a number of loop configurations reflecting the scenarios to be expected in real deployments. Tables specify the primary parameters for the insertion loss of the underlying elementary loops.

The efforts regarding crosstalk modeling have been focused mainly on predicting the resulting power spectral density in a victim pair caused by a number of crosstalkers active in neighboring pairs^{8,18,19}. A verification and refinement of these models is reported in²⁰.

Measurement results up to 30MHz have been presented in²¹⁻²³. Further measurements in the frequency range up to 30MHz focusing on various aspects of different DSL technologies are reported in²⁴⁻³².

None of the works discussed above explores the possibility of using the copper loops for DSL transmission in frequency bands above 30MHz. To fill this gap, several key aspects of the copper media transmission performance in frequency bands above 30MHz need to be studied in detail and duly clarified. One of these aspects is the characterization of insertion loss and crosstalk coupling for such high frequency bands. In this paper we present the first results of an ongoing effort to characterize, through systematic measurements of the insertion loss and crosstalk coupling functions, very short copper loops in a length range from 50m to 200m and in a frequency band from 100kHz to 200MHz. Moreover, the results of the measurements are compared with the simulation results obtained by extrapolating the most commonly used insertion loss and crosstalk coupling models described in the next section.

2.2. Reference models used for extrapolation and comparison

For insertion loss we use the simple high-frequency approximation of the propagation-constant based description given in¹. The insertion-loss function for a 0.4 mm-loop[†] can be written as

$$H_{IL}(f, L) = e^{-L/L_{\text{mile}}k_1\sqrt{f} + k_2f - jL/L_{\text{mile}}k_3f} \quad \text{with} \quad L_{\text{mile}} = 1609.344\text{m}, k_1 = 4.8e^{-3}, k_2 = -1.709e^{-8}, k_3 = 4.907e^{-5} \quad (1)$$

where f is the frequency in Hz and L is the length of the loop in m.

For the magnitude of NEXT and FEXT coupling functions we use the models proposed by ETSI¹⁹.

The FEXT coupling function can be written as

$$H_{\text{FEXT}}(f, L) = k_{\text{XF}} f / f_0 \sqrt{L/L_0} |H_{IL}(f, L)| \quad \text{with} \quad f_0 = 1\text{MHz}, L_0 = 1\text{km}, k_{\text{XF}} = 10^{-45/20}. \quad (2)$$

The NEXT coupling function is given by

$$H_{\text{NEXT}}(f, L) = k_{\text{XN}} (f/f_0)^{3/4} \sqrt{1 - |H_{IL}(f, L)|^4} \quad \text{with} \quad f_0 = 1\text{MHz}, k_{\text{XN}} = 10^{-50/20}. \quad (3)$$

Note that the ETSI models for NEXT and FEXT do not provide phase information.

[†] A wire diameter of 0.4 mm corresponds to the American wire gauge (AWG) designation AWG26.

3. MEASUREMENT SETUP

The transfer functions and coupling functions are measured directly in frequency-domain using a gain/phase-analyzer, which sweeps a sinusoid through a grid of specified frequencies and determines the relative gain and the phase difference with respect to the signal present at its reference input. Table 1 summarizes the gain/phase-analyzer settings used for the measurements presented hereinafter.

Cables of the following type were measured:

- Cable No. 1: 200m EULEV 10x2x0.4 TEH 240 1402/010 on drum
- Cable No. 2: 50m EULEV 10x2x0.4 TEH 240 1402/010 wrapped to a ring with a mean diameter of 0.55m

A list of the employed laboratory equipment is included in the appendix.

Start frequency	100 kHz
Stop frequency	200 MHz
No. of points	801
Averaging	32-fold
IF-bandwidth	30 kHz
Channel 1 settings	A/R, LOG MAG, source power: 0 dBm
Channel 2 settings	A/R, PHASE (RAD), source power: 0 dBm
Sweep time	352.4 ms
Sweep type	LIN FREQ

Table 1. Gain/phase-analyzer parameters

4. MEASUREMENT RESULTS AND COMPARISON WITH EXTRAPOLATED 30MHZ-MODELS

4.1. Stability and reproducibility of UWB measurements

As the frequency band spanned by the measurements grows, the common concern regarding stability and reproducibility of the results increases. In order to quantify the reliability of our results, we have repeated a set of single-pair measurements. While the environmental conditions such as temperature or humidity remained constant[‡], the connection of the different elements in the measurement setup and the calibration of the gain/phase-analyzer have been redone before each individual measurement.

Figure 1, Figure 2, and Figure 3 depict insertion loss, FEXT coupling function and NEXT coupling function for the 50m-cable, respectively. Each figure shows the mean value and the corresponding 95% confidence interval. Except for some frequencies corresponding to deep dips in the magnitude response, the results can be considered stable over the whole frequency band. The exact value of the measured results in these dips is of low relevance for two reasons. First, the measured magnitude responses exhibit low values compared to other frequency ranges. Thus, the contribution of these narrow frequency bands corresponding to magnitude-dips to the overall throughput is marginal and the exact value of the magnitude response at such a dip-frequency is of vanishing significance. Second, the deviations in the results are mainly a consequence of limitations in the precision of the measurement setup.

Figure 4, Figure 5, and Figure 6 depict insertion loss, FEXT coupling function and NEXT coupling function for the 200m-cable, respectively. Around 150MHz the phase results of all three parameters begin to flatten out. This effect is visible only for the 200m-measurements presented in this paper—we have observed the same behavior for the 50m piece at frequencies way above 200MHz. The results suggest that we meet the background-noise level of the setup at this frequency or parasitic effects and coupling mechanisms begin to dominate. For the 200m-cable, we suggest to limit the frequency range within which we obtain trustworthy measurement results to around 100MHz. Table 2 summarizes the maximum 95% confidence interval value over frequency.

[‡]The measurements were carried out in a climatized laboratory.

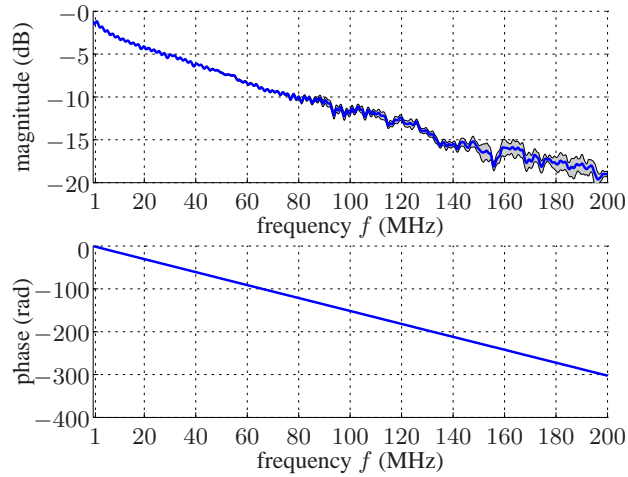


Figure 1. 50m-cable: mean insertion loss and 95% confidence interval.

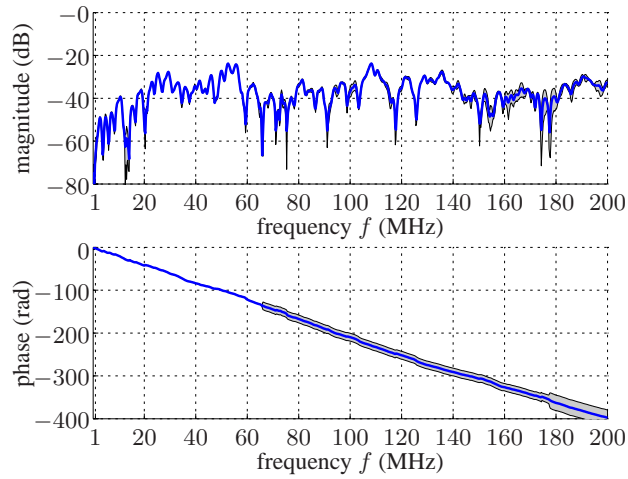


Figure 2. 50m-cable: mean FEXT and 95% confidence interval.

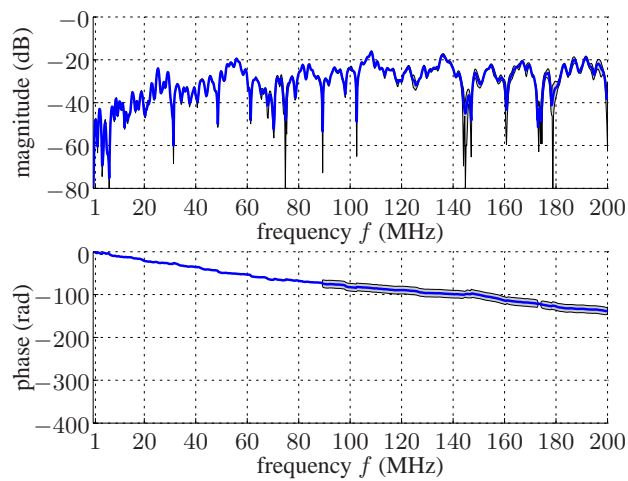


Figure 3. 50m-cable: mean NEXT and 95% confidence interval.

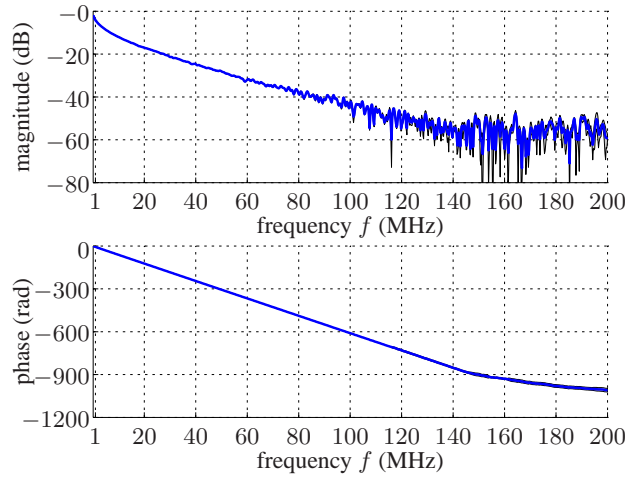


Figure 4. 200m-cable: mean insertion loss and 95% confidence interval.

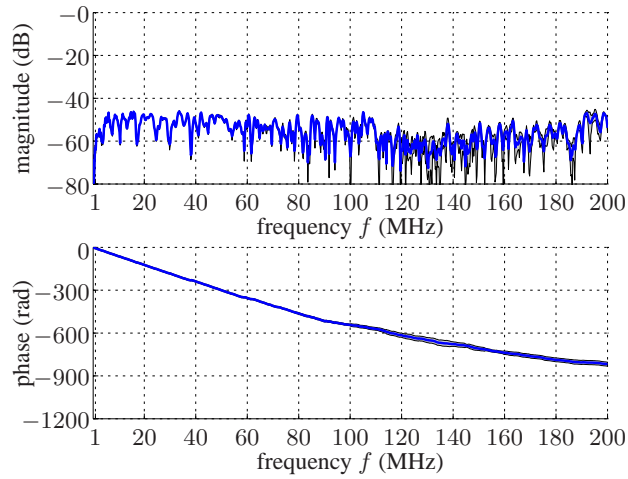


Figure 5. 200m-cable: mean FEXT and 95% confidence interval.

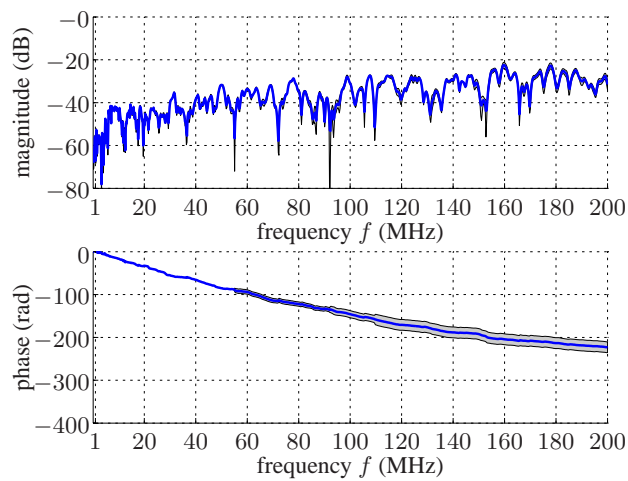


Figure 6. 200m-cable: mean NEXT and 95% confidence interval.

50m-cable, insertion loss, magnitude	1.1 dB
50m-cable, insertion loss, phase	0.2 rad
50m-cable, FEXT, magnitude	3.9 dB
50m-cable, FEXT, phase	18.3 rad
50m-cable, NEXT, magnitude	4.1 dB
50m-cable, NEXT, phase	10.3 rad
200m-cable, insertion loss, magnitude	0.03 dB
200m-cable, insertion loss, phase	13.0 rad
200m-cable, FEXT, magnitude	5.1 dB
200m-cable, FEXT, phase	20.7 rad
200m-cable, NEXT, magnitude	1.6 dB
200m-cable, NEXT, phase	13.2 rad

Table 2. Maxima of absolute of 95% confidence intervals over the whole frequency range (50m-cable: 100kHz–200MHz; 200m-cable: 100kHz-100MHz)

4.2. Long-term variations of UWB cable properties

Although copper cable properties are in general considered time invariant, it is imperative to verify this assumption for high-frequency ranges. In order to characterize possibly existing time variations, a series of measurements of a FEXT coupling function has been carried out. For each of the two cables, around 10000 measurements of the coupling function have been taken in a time interval of around 20 hours. Note that the measurement setup has not been touched during these measurements, which is the fundamental difference compared to the reproducibility measurements described in the previous section. Figure 7 and Figure 8 depict the mean values of the FEXT coupling function over the measurement ensemble for the 50m-cable and the 200m-cable[§], respectively. Additionally, the minimum and the maximum measured results are shown (gray-shaded areas). Table 3 summarizes the maximum 95% confidence interval value over frequency.

50m-cable, magnitude	0.2 dB
50m-cable, phase	0.7 rad
200m-cable, magnitude	0.5 dB
200m-cable, phase	0.2 rad

Table 3. Maxima of absolute of 95% confidence intervals over the whole frequency range (50m-cable: 100kHz–200MHz; 200m-cable: 100kHz-100MHz)

4.3. Comparison with extrapolated 30MHz-models

Figure 9, Figure 10, and Figure 11 depict the ensemble average of measured insertion loss, FEXT, and NEXT, respectively, together with the corresponding modeling results for the 50m-cable. In general, the match between the insertion loss model and the measured results is reasonable—although the model appears a bit too conservative for frequencies below 140MHz and slightly too optimistic for frequencies above 140MHz. The extrapolated ETSI models provide reasonable worst-case results for both FEXT and NEXT.

Figure 12, Figure 13, and Figure 14 depict the ensemble average of measured insertion loss, FEXT, and NEXT, respectively, together with the corresponding modeling results for the 200m-cable. The extrapolated model is a bit too pessimistic for insertion loss. For FEXT in the 200m-cable, we conclude that the ETSI model provides a good worst-case magnitude of the coupling function. For NEXT in the 200m-cable, the ETSI model seems to be a bit too conservative.

[§]Note that the long-term experiments have been carried out for a different pair-set compared to the reproducibility-experiments presented in the previous section.

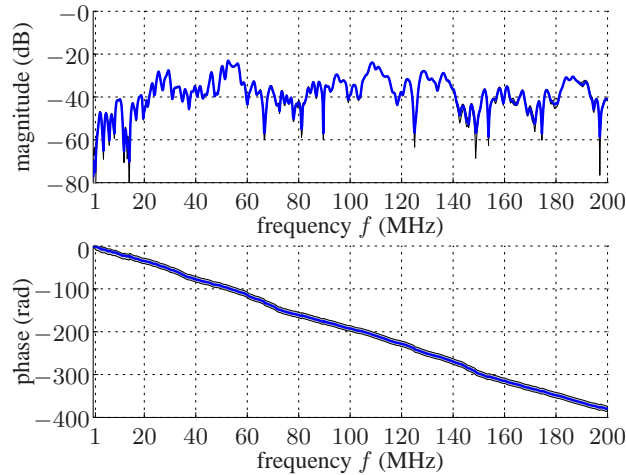


Figure 7. 50m-cable, long-term measurements: FEXT coupling function ensemble mean (corresponds to mean over time) and minimum/maximum range (gray-shaded fields).

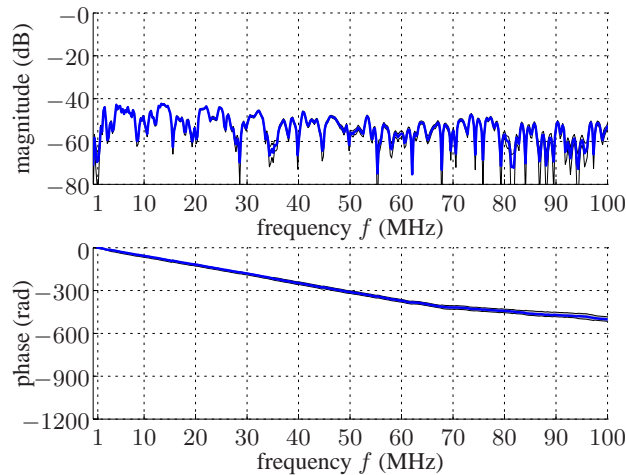


Figure 8. 200m-cable, long-term measurements: FEXT coupling function ensemble mean (corresponds to mean over time) and minimum/maximum range (gray-shaded fields).

5. DISCUSSION AND CONCLUSIONS

This paper presents measurement results of insertion loss and crosstalk coupling properties of short copper cables for frequencies beyond 30MHz. In general, we observe a reasonable match between the measurement results and the extrapolated 30MHz models. The phase of the insertion loss flattens out at 'high' frequencies—this might be an indicator for the frequency where we should stop to measure/model—at least with the equipment at hand. This effect is visible only for the 200m-measurements presented in this paper—we have observed the same behavior for the 50m-piece at frequencies way above 200MHz.

For the 50m-cable, the match between the insertion loss model and the measured results is reasonable—although the model appears a bit too conservative for frequencies below 140MHz and slightly too optimistic for frequencies beyond 140MHz. The extrapolated ETSI models provide reasonable worst-case results for both FEXT and NEXT. For the 200m-cable, the extrapolated model is too pessimistic for insertion loss. For FEXT in the 200m-cable, although the ETSI-model provides a good-worst case prediction, a flat coupling function for high frequencies seems to be more realistic than a coupling function that decreases with loop attenuation (like the standard 30MHz FEXT model). For NEXT in the 200m-cable, the ETSI model seems to be a bit too conservative.

Finally, we would like to emphasize that the results of this contribution reflect the status of ongoing work which is to be finished before inferring definitive conclusions.

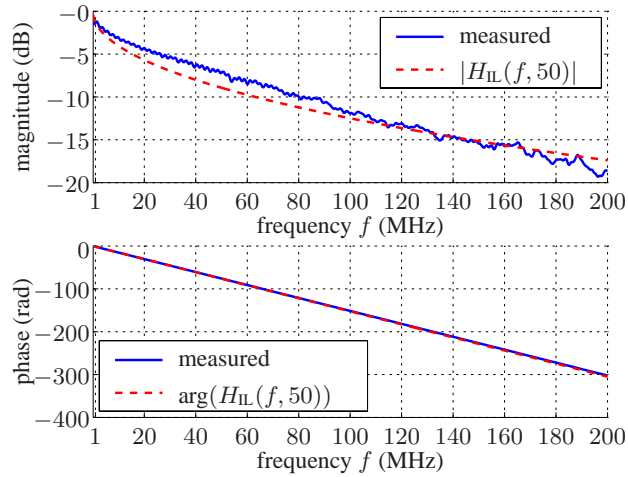


Figure 9. 50m-cable, insertion loss: ensemble mean and extrapolated Chen-model (1).

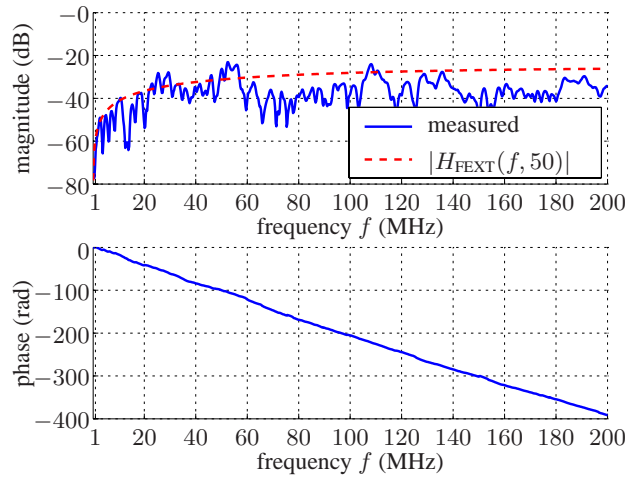


Figure 10. 50m-cable, FEXT: ensemble mean and extrapolated ETSI-model (2).

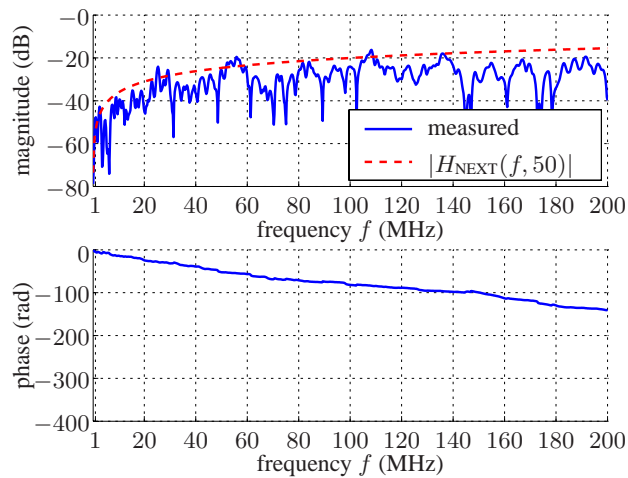


Figure 11. 50m-cable, NEXT: ensemble mean and extrapolated ETSI-model (3).

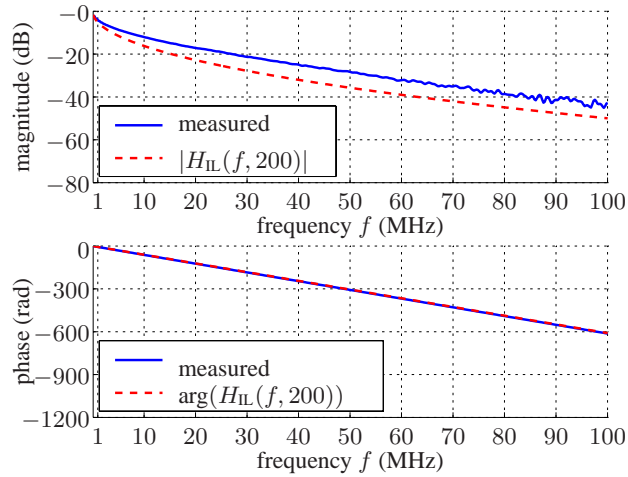


Figure 12. 200m-cable, insertion loss: ensemble mean and extrapolated Chen-model (1).

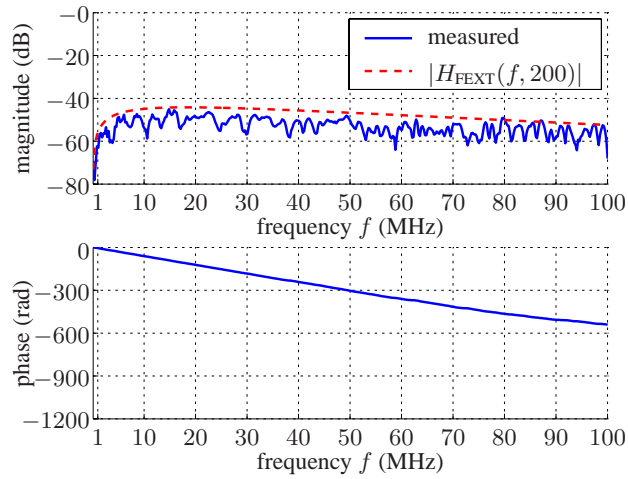


Figure 13. 200m-cable, FEXT: ensemble mean and extrapolated ETSI-model (2).

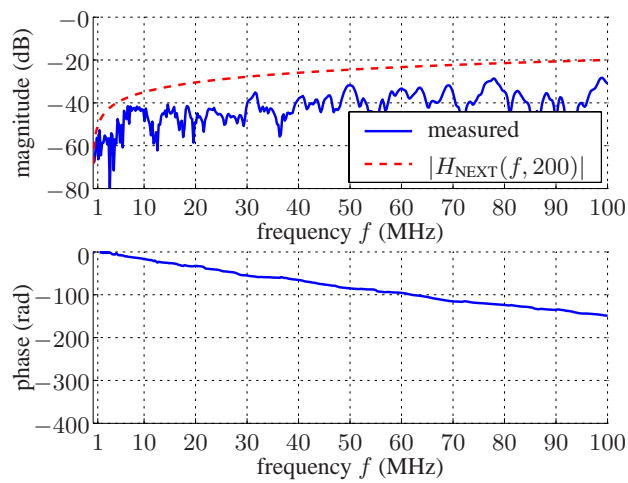


Figure 14. 200m-cable, NEXT: ensemble mean and extrapolated ETSI-model (3).

6. ACKNOWLEDGMENTS

The authors would like to thank Henrik Almeida for support and coordinating the effort during the work. We are grateful to Klas Ericson for his support in the lab and his valuable feedback during numerous discussions. We acknowledge the financial support received from the European Commission IST 6th Framework and from the Swedish Agency for Innovation Systems, VINNOVA, through the IST-MUSE and the Eureka-Celtic BANITS projects respectively, which partially enabled this work. We acknowledge the financial support received from FAPESP-Brazil.

7. APPENDIX: LABORATORY SETUP—EMPLOYED EQUIPMENT

- Network analyzer: 1 Agilent 4395A
- Baluns: 2 North Hills NH14833 (10MHz–600MHz, 50Ohm UNB, 100Ohm BAL), serial number: SN0809/DC0547 (device No. 1), SN0810/DC0547 (device No. 2)
- Signal splitter: Agilent 87512A DC-2 GHz
- Cable No. 1: 200m EULEV 10x2x0.4 TEH 240 1402/010 on drum
- Cable No. 2: 50m EULEV 10x2x0.4 TEH 240 1402/010 wrapped to a ring with a mean diameter of 0.55m

REFERENCES

1. W. Y. Chen, *DSL: Simulation Techniques and Standards Development for Digital Subscriber Line Systems*, Macmillan Technical Publishing, ISBN 1-57870-017-5, 1998.
2. ITU-T, “G.selt: Updated issues list for G.selt,” *ITU-T Temporary Document SS U09*, 2004.
3. ITU-T, “Asymmetric digital subscriber line (ADSL) transceivers,” *ITU Recommendation G.992.1*, June 1999.
4. ITU-T, “Asymmetric digital subscriber line (ADSL) transceivers,” *ITU Recommendation G.992.2*, June 1999.
5. ITU-T, “Asymmetric digital subscriber line (ADSL) extended bandwidth (ADSL2+),” *ITU Recommendation G.992.5*, 2005.
6. T. Starr, J. M. Cioffi, and P. Silverman, *Understanding Digital Subscriber Line Technology*, Prentice Hall, Englewood Cliffs, 1998.
7. H. Dedieu, *Fundamentals of DSL Technology*, ch. ‘The Copper Channel—Loop Characteristics and Models’. ISBN 0849319137, AUERBACH, 2005.
8. R. F. M. van der Brink, “Cable reference models for simulating metallic access networks,” Permanent Document TM6(97), ETSI STC TM6, Luleå, Sweden, June 1998.
9. C. R. Paul, *Analysis of Multiconductor Transmission Lines*, Wiley, ISBN 0-471-02080-X, 1994.
10. J. W. Cook, “Parametric modelling of twisted pair cables for VDSL,” Temporary Document TD22, ETSI STC TM6, Vienna, Austria, Mar. 1996.
11. R. F. M. van der Brink, “Measurements and models on Dutch cables,” Temporary Document TD15, ETSI STC TM6, Tel Aviv, Israel, Mar. 1997.
12. M. Pollakowski, “DTAG cables transmission characteristics,” Temporary Document TD40, ETSI STC TM6, Vienna, Austria, Mar. 1996.
13. F. Pythoud, “Model of Swiss access network cables,” Temporary Document TD48, ETSI STC TM6, Madrid, Spain, Jan. 1998.
14. L. Heylen and J. Musson, “Cable models predict physically impossible behavior in time domain,” Temporary Document TD08, ETSI STC TM6, Amsterdam, Netherlands, Nov. 1999.
15. J. Musson, “Maximum likelihood estimation of the primary parameters of twisted pair cables,” Temporary Document TD06, ETSI STC TM6, Madrid, Spain, Sept. 1998.
16. P. Boets, M. Zekri, L. van Biesen, T. Bostoen, and T. Pollet, “On the identification of cables for metallic access networks,” in *18th IEEE Instrumentation and Measurement Technology Conference IMTC2001*, 2, pp. 1348–1353, (Budapest, Hungary), May 2001.
17. T. Bostoen, P. Boets, M. Zekri, L. van Biesen, T. Pollet, and D. Rabijns, “Estimation of the transfer function of the access network by means of one-port scattering parameter measurements at the central office,” *IEEE Journal on Selected Areas in Communication* 20, pp. 936–948, June 2002.
18. ANSI T1E1.4, “Very-high-bit-rate Digital Subscriber Line (VDSL) Metallic Interface Part 1: Functional Requirement and Common Specification,” *T1E1.4/2000-009R3*, Feb. 2001.
19. R. F. M. van der Brink, “Laboratory performance tests for xDSL systems,” Permanent Document TM6(98)10, ETSI STC TM6, Sophia Antipolis, France, Feb. 2001.
20. C. Valenti, “NEXT and FEXT Models for Twisted-Pair North American Loop Plant,” *IEEE Journal on Selected Areas in Communication* 20, pp. 893–900, June 2002.
21. N. H. Nedev, S. McLaughlin, and J. W. Cook, “Wideband UTP Cable Measurements And Modelling for MIMO Systems,” in *Proc. European Signal Processing Conf. EUSIPCO 2004*, (Vienna, Austria), Sept. 2004.

22. T. Magesacher, W. Henkel, G. Tauböck, and T. Nordström, "Cable Measurements Supporting xDSL Technologies," *Journal e&i Elektrotechnik und Informationstechnik* **199**, pp. 37–43, Feb. 2002.
23. T. Magesacher, P. Ödler, P. O. Börjesson, W. Henkel, T. Nordström, R. Zukunft, and S. Haar, "On the Capacity of the Copper Cable Channel Using the Common Mode," in *Proc. IEEE Global Telecommun. Conf. GLOBECOM 2002*, (Taipei, Taiwan), Nov. 2002.
24. N. Tomita and M. Ohmura, "Low-frequency crosstalk loss characteristics of balanced cables," *Electron. Commun. Japan, part 1* **72**(3), pp. 95–105, 1989.
25. J. J. Goedbloed, "Aspects of EMC at the equipment level," in *Proc. 12th Intl. Symp. Electromagn. Compat.*, pp. 23–38, (Zurich, Switzerland), Feb. 1997.
26. J. J. Werner, "The HDSL Environment," *IEEE Journal on Selected Areas in Communication* **9**, pp. 785–800, Aug. 1991.
27. R. A. Conte, "A crosstalk model for balanced digital transmission in multipair cables," *AT&T Tech. J.* **65**, pp. 41–59, May-Jun 1986.
28. J. E. Schutt-Ainé, "High-Frequency Characterization of Twisted-Pair Cables," *IEEE Trans. on Commun.* **49**, pp. 598–601, Apr. 2001.
29. P. A. Gresh, "Physical and transmission characteristics of customer loop plant," *The Bell System Technical Journal* **48**, pp. 3337–3385, Dec. 1969.
30. L. M. Manhire, "Physical and transmission characteristics of customer loop plant," *The Bell System Technical Journal* **57**, pp. 35–39, Jan. 1978.
31. S. B. Pierce, "Crosstalk in twisted pair circuits," in *Proc. Intl. Wire and Cable Symp.*, pp. 349–354, 1986.
32. A. Fung, L. S. Lee, and D. D. Falconer, "A facility for near end crosstalk measurements on ISDN subscriber loops," in *Proc. IEEE Global Telecommun. Conf.*, 1989, paper 54.1.